

# Hydrido(1,4,8,11,15,18,22,25-octa-*n*-pentylphthalocyaninato)-rhodium Dimers: Single-Crystal X-ray Structure and the Isomerization of the Four Isomers<sup>†</sup>

M. J. Chen,\* L. Nuñez,\* and J. W. Rathke

Chemical Technology Division, Argonne National Laboratory, 9700 South Cass Avenue, Argonne, Illinois 60439

R. D. Rogers

Department of Chemistry, Northern Illinois University, DeKalb, Illinois 60115

Received November 27, 1995<sup>⊗</sup>

The hydrido(phthalocyaninato)rhodium dimer [(R<sub>8</sub>Pc)RhH]<sub>2</sub> (**1**; R<sub>8</sub>Pc<sup>2-</sup> = dianion of 1,4,8,11,15,18,22,25-octa-*n*-pentylphthalocyanine) was synthesized from the reaction of [(R<sub>8</sub>Pc)(MeOH)<sub>2</sub>Rh]Cl with H<sub>2</sub> at 110 °C in 1-pentanol. A single-crystal X-ray diffraction study shows that **1** is a dimer. The two Pc ligands are essentially planar and staggered by 35(2)°. The two Rh atoms are not significantly displaced from the planes of the ligands; they are separated by 3.347(3) Å. This long Rh–Rh separation suggests that **1** has a bridging hydride ligand. The dimeric structure of **1** is maintained in benzene solution. The <sup>1</sup>H NMR spectra show that **1** contains one Rh–H and one N–H moiety for every two R<sub>8</sub>Pc<sup>2-</sup> ligands. The ν<sub>NH</sub> band at 3373 cm<sup>-1</sup> (the ν<sub>ND</sub> band at 2478 cm<sup>-1</sup>) supports the presence of an N–H moiety in **1**. Our belief that protonation occurs on a *meso* (or peripheral) nitrogen, rather than a pyrrolic nitrogen, is derived from X-ray structural data and <sup>1</sup>H NMR results. (1) No uniquely long Rh–N bond is present, and all four pyrrolic nitrogens remain on the same plane, along with the Rh atom. (2) The chemical shift of δ 11.6 ppm for the N–H proton indicates that it is highly deshielded and, therefore, lies outside the extended ring currents of the Pc ligand. Therefore, the hydride-bridged isomer (R<sub>8</sub>PcH)Rh(*μ*-H)Rh(R<sub>8</sub>Pc) (**1a**), in which the proton of R<sub>8</sub>PcH<sup>-</sup> resides on a *meso* nitrogen, is proposed for **1** in the solid state and in benzene solution. Variable-temperature <sup>1</sup>H NMR studies of **1** in toluene-*d*<sub>8</sub> indicate that when *T* ≥ 115 °C, **1** dissociates into the monomeric hydride complex (R<sub>8</sub>Pc)RhH (**2**); when *T* ≤ -25 °C, four isomers of **1**, all of which have one Rh–H and one N–H moiety, are reversibly formed. Two isomers (**1b** and **1c**), which exhibit fine structure in the hydride resonance due to their coupling to two inequivalent Rh nuclei, are assigned to two rotamers of the terminal hydride dimer (R<sub>8</sub>PcH)RhRh(R<sub>8</sub>Pc)H. The fourth isomer (**1d**), which is the only isomer present at -85 °C, is assumed to be another hydride-bridged dimer, i.e., a rotamer of **1a**.

## Introduction

Although metallophthalocyanines (MPc's) have been investigated as catalysts for the oxidation of hydrocarbons and other organic substrates,<sup>1</sup> their organometallic chemistries have rarely been explored. We have been able to find only a very limited number of alkyl and aryl complexes of MPc's reported<sup>2</sup> and even fewer hydride complexes of MPc's. To our knowledge, [(R<sub>8</sub>Pc)RhH]<sub>2</sub>

(**1**; R<sub>8</sub>Pc<sup>2-</sup> = dianion of 1,4,8,11,15,18,22,25-octa-*n*-pentylphthalocyanine) and (R<sub>8</sub>Pc)RhH (**2**), which we reported earlier,<sup>3</sup> are still the only known hydride complexes of MPc's. Here we report a single-crystal X-ray structure which confirms the dimeric structure of **1**, and variable-temperature <sup>1</sup>H NMR studies which show that **1** dissociates into **2** at high temperatures and that four isomers of **1** are reversibly formed at low temperatures. These results also suggest that the N–H proton of **1** resides on a *meso* (or peripheral) nitrogen, rather than a pyrrolic nitrogen. The structures of these isomers are discussed.

## Results

**Synthesis and Characterization of [(R<sub>8</sub>Pc)RhH]<sub>2</sub> (**1**).** The synthesis of [(R<sub>8</sub>Pc)RhH]<sub>2</sub> by reaction of [(R<sub>8</sub>Pc)(MeOH)<sub>2</sub>Rh]Cl with H<sub>2</sub> in 1-pentanol at 110 °C has been described.<sup>3</sup> The <sup>1</sup>H NMR spectra of **1** in toluene-*d*<sub>8</sub> show that it has one Rh–H resonance at δ -38.1 ppm and one N–H resonance at δ 11.6 ppm for every two

<sup>†</sup> Work supported by the U.S. Department of Energy, Division of Chemical Sciences, Office of Basic Energy Sciences, under Contract No. W-31-109-ENG-38.

<sup>⊗</sup> Abstract published in *Advance ACS Abstracts*, April 1, 1996.

(1) (a) Moser, F. H.; Thomas, A. L. *The Phthalocyanines*; CRC Press: Boca Raton, FL, 1983. (b) Nappa, M. J.; Tolman, C. A. *Inorg. Chem.* **1985**, *24*, 4711. (c) Lyons, J. E.; Ellis, P. E., Jr. *Appl. Catal. A* **1992**, *84*(2), L1. (d) Herron, N.; Stucky, G. D.; Tolman, C. A. *J. Chem. Soc., Chem. Commun.* **1986**, *20*, 1521. (e) Herron, N. *J. Coord. Chem.* **1988**, *19*, 25. (f) Parton, R. F.; Vankelecom, I. F. J.; Casselman, M. J. A.; Bezoukhanova, C. P.; Uytterhoeven, J. B.; Jacobs, P. A. *Nature* **1994**, *370*, 541.

(2) (a) Taube, R.; Drevs, H.; Hiep, T. D. *Z. Chem.* **1969**, *9*, 115. (b) Vol'pin, M. E.; Taube, R.; Drevs, H.; Volkova, L. G.; Levitin, I. Y. A.; Ushakova, T. M. *J. Organomet. Chem.* **1972**, *39*, C79. (c) Day, P.; Hill, H. A. O.; Price, M. G. *J. Chem. Soc. A* **1968**, 90. (d) Galezowski, W.; Ibrahim, P. N.; Lewis, E. S. *J. Am. Chem. Soc.* **1993**, *115*, 8660. (e) Chen, M. J.; Rathke, J. W.; Huffman, J. C. *Organometallics* **1993**, *12*, 4673.

(3) Chen, M. J.; Rathke, J. W. *J. Chem. Soc., Chem. Commun.* **1992**, 309.

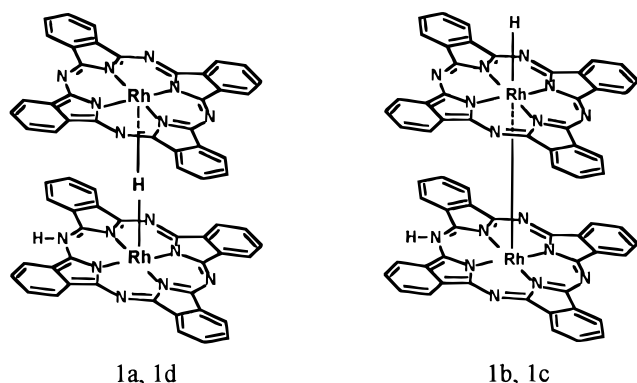


**Figure 1.** Schematic drawings of the proposed isomers of  $[(C_5H_{11})_8Pc]RhH)_2$ . The pentyl groups are omitted for clarity.



**Figure 2.** ORTEP drawing of  $[(C_5H_{11})_8PcRhH)_2$ . The pentyl chains have been represented as lines for clarity.

$(R_8Pc)^{2-}$  ligands. The presence of the N–H bond in **1** was further supported by IR spectra, which give the  $\nu_{N-H}$  band at  $3373\text{ cm}^{-1}$  (the  $\nu_{N-D}$  band is at  $2478\text{ cm}^{-1}$ ) for the KBr pellet and  $3385\text{ cm}^{-1}$  for the benzene solution. No IR band attributable to the terminal Rh–H or the bridging Rh–H–Rh was observed. On the basis of these spectral data, we previously suggested the terminal hydride isomer  $(R_8PcH)Rh-Rh(R_8Pc)H$  for **1** in the solid state and in benzene.<sup>3,4</sup> However, the results from the single-crystal X-ray diffraction study and the variable-temperature  $^1H$  NMR study, described in the following sections, lead us to believe that the molecular structure of **1** in the solid state, as well as in benzene at ambient temperature, is the hydride-bridged isomer  $(R_8PcH)Rh(\mu-H)Rh(R_8Pc)$  (**1a**), in which the N–H proton of  $R_8PcH^-$  resides on a *meso* nitrogen.

**Molecular Structure of  $[(R_8Pc)RhH)_2$  in the Solid State.** The crystal data and structure refinement for  $[(R_8Pc)RhH)_2$  are shown in Table 1. The crystal, obtained from a benzene solution, belongs to the centric space group  $C2/c$ . High thermal motion was noted for the last two to four carbon atoms in each  $n-C_5H_{11}$  chain. Disorder was resolvable only for one carbon atom of the  $n-C_5H_{11}$  chains, which was refined in two positions at 50% occupancy each in alternate least-squares cycles. Because of high thermal motion and disorder, the hydrogen atoms were not included in the final refine-

**Table 1. Crystal Data and Structure Refinement for the  $[(R_8Pc)RhH)_2$  Complex**

compd	$[(n-C_5H_{11})_8PcRhH)_2$
color/shape	dark purple/thin plate
empirical formula	$C_{72}H_{97}N_8Rh$
fw	1179.50
temp	293(2) K
cryst syst	monoclinic
space group	$C2/c$
unit cell dimens	$a = 36.579(2)\text{ \AA}$ $b = 19.312(1)\text{ \AA}$ $c = 18.772(2)\text{ \AA}$ $\alpha = 90^\circ$ $\beta = 101.08(4)^\circ$ $\gamma = 90^\circ$
$V$	$13014(2)\text{ \AA}^3$
$Z$	8
density (calcd)	$1.204\text{ Mg/m}^3$
abs coeff	$0.310\text{ mm}^{-1}$
diffractometer	Rigaku R-Axis II area detector
radiation/wavelength	Mo K $\alpha$ (graphite monochrom) $0.710\text{ 37 \AA}$
$F(000)$	5056
cryst size	$1.00 \times 0.10 \times 0.040\text{ mm}$
$\theta$ range for data collec	$1.55-17.65^\circ$
index ranges	$0 \leq h \leq 31, -16 \leq k \leq 16,$ $-15 \leq l \leq 13$
no. of rflns collected	20 000
no. of indep rflns	3811 ( $R_{int} = 0.073$ )
refinement methods	full-matrix-block least-squares on $F^2$
computing	SHELXS-86, SHELX-93
no. of data/restraints/params	3777/58/649
goodness of fit on $F^2$	1.084
SHELX-93 weight params	0.14, 100
final $R$ indices ( $I > 2\sigma(I)$ )	$R1 = 0.0777, wR2 = 0.2099$
$R$ indices (all data)	$R1 = 0.0881, wR2 = 0.2445$
largest diff peak and hole	$0.731$ and $-0.360\text{ e \AA}^{-3}$

ment. Refinement of non-hydrogen atoms with anisotropic temperature factors (except as noted in the Experimental Section) led to the final  $R$  value of 0.078.

An ORTEP diagram of **1** is shown in Figure 2. The two Pc ligands are essentially planar and are staggered by  $35(2)^\circ$ . The two Rh atoms are not significantly displaced from the planes of the ligands. They are separated by  $3.347(3)\text{ \AA}$ , which is definitely too long for an unsupported Rh(II)–Rh(II) dimer and may be even too long for an unsupported Rh(I)–Rh(I) dimer. Typical Rh–Rh bond lengths in unsupported Rh(II)–Rh(II) and Rh(I)–Rh(I) dimers are shown in Table 2.<sup>5,6</sup> Formally, **1** may be considered as a mixed-valence Rh(I)–Rh(III) dimer, i.e., a dimer formed by joining together  $(R_8PcH)Rh$  and  $(R_8Pc)RhH$ . The Rh–Rh separation of  $3.347\text{ \AA}$  is definitely too long for the Rh–Rh-bonded isomers **1b** and **1c**. We, therefore, believe that isomer **1a**, a dimer with a protonated *meso* nitrogen and a bridging hydride ligand, is the molecular structure for **1** in the solid state.

Protonation is believed to occur on a *meso* nitrogen because there is no uniquely long Rh–N bond, and the Rh atom and all four pyrrolic nitrogens in  $(R_8PcH)Rh$  rest on a plane. In all of the N-alkylated porphyrins

(5) (a) Caulton, K. G.; Cotton, F. A. *J. Am. Chem. Soc.* **1969**, *93*, 1914. (b) Warren, L. F.; Dehaven, P. W.; Goedken, V. L. Unpublished results. (c) Olmsted, M. M.; Balch, A. L. *J. Organomet. Chem.* **1978**, *148*, C15. (d) Fonseca, E.; Gelger, W. E.; Bitterwolf, T. E.; Rheingold, A. L. *Organometallics* **1988**, *7*, 567. (e) Dunbar, K. R. *J. Am. Chem. Soc.* **1988**, *110*, 8247. (f) Kuz'menko, I. V.; Golubnichaya, M. A.; Baranovskii, I. B. *Zh. Neorg. Khim.* **1991**, *36*, 164. (g) Dikareva, L. M.; Andrianov, V. I.; Zhilyaev, A. N.; Baranovskii, I. B. *Zh. Neorg. Khim.* **1989**, *34*, 430. (h) Dikareva, L. M.; Andrianov, V. I.; Zhilyaev, A. N.; Baranovskii, I. B. *Zh. Neorg. Khim.* **1989**, *34*, 391.

(6) Mann, K. R.; Lewis, N. S.; Williams, R. M.; Gray, H. B.; Gordon, J. G., II. *Inorg. Chem.* **1978**, *17*, 828.

(4) Chen, M. J.; Rathke, J. W. *Organometallics* **1994**, *13*, 4875.

**Table 2. Structural Data for Dinuclear Rhodium Compounds without Bridging Ligands**

compd	$r(\text{Rh}-\text{Rh})$ , Å	ref
Rh(II)-Rh(II) dimers		
$[\text{Rh}(\text{DMG})_2(\text{PPh}_3)]_2\text{C}_3\text{H}_7\text{OH}\cdot\text{H}_2\text{O}$	2.936(2)	5a
$[\text{Rh}(\text{p-CH}_3\text{C}_6\text{H}_4\text{NC})_4\text{I}]_2(\text{PF}_6)_2$	2.785(2)	5c
$[\text{RhCp}(\text{CO})\text{P}(\text{OPh})_3]_2(\text{PF}_6)_2$	2.814(1)	5d
$[\text{Rh}(\text{CH}_3\text{CN})_5]_2$	2.624(1)	5e
$[\text{Rh}(\text{C}_{22}\text{H}_{22}\text{N}_4)]_2\cdot 3\text{C}_6\text{H}_6^a$	2.625(2)	5b
$[\text{Rh}(\text{DMG})_2(\text{py})]_2$	2.726(1)	5f
$[\text{Rh}(\text{hfacac})_2(\text{py})]_2^b$	2.590(1)	5g
$[\text{Rh}(\text{CH}_3\text{CN})_4(\text{H}_2\text{O})]_2$	2.655(1)	5h
Rh(I)-Rh(I) Dimer		
$[\text{Rh}(\text{CNC}_6\text{H}_5)_4]_2^{2+}$	3.193(0)	6

<sup>a</sup>  $(\text{C}_{22}\text{H}_{22}\text{N}_4)^{2-} = 7,16$ -dihydro-6,8,15,17-tetramethyldibenzo[*b,h*]-1,4,8,11-tetraazacyclotetradecinate. <sup>b</sup> hfacac = heptafluoroacetyl-acetate ion.

for which the structures have been determined by single-crystal X-ray diffraction, the Rh-N bond of the alkylated nitrogen is 0.2–0.4 Å longer than those of the other pyrrolic nitrogens.<sup>7</sup> The lengthening of this Rh-N bond, which is accompanied by tilting of the pyrrole ring, is attributed to the ineffective bonding between the Rh and the rehybridized  $\text{sp}^3$  nitrogen. Distortion of 19.1° of the alkylated nitrogen from the plane defined by the other three nitrogens has also been reported for a nonmetalated *N*-alkylporphyrin.<sup>8</sup>

**Variable-Temperature <sup>1</sup>H NMR Study of [(R<sub>8</sub>Pc)-RhH]<sub>2</sub> in Toluene-*d*<sub>8</sub>.** The presence of a bridging hydride ligand in the crystal of **1**, as suggested by the single-crystal X-ray diffraction study, prompted us to extend our <sup>1</sup>H NMR study of **1** to low temperatures to search for additional evidence for the bridging hydride ligand.

**(A) Ambient Temperatures.** Figure 3a shows that the toluene-*d*<sub>8</sub> solution of **1** at ambient temperature has one N-H resonance at  $\delta$  11.6 ppm and one Rh-H resonance at  $\delta$  -38.1 ppm for each Rh dimer. The alkyl and aryl resonances (Figure 4) are complicated, but they may be separated into two groups of roughly equal combined intensities. The group with sharper and better defined resonances is marked with asterisks in Figure 4a and is assigned to the half of the dimer that has the Rh-H moiety, i.e., the (R<sub>8</sub>Pc)RhH macrocycle. The rest of the resonances, which are more diffuse, are assigned to the half of the dimer with one of its *meso* nitrogens protonated, i.e., the (R<sub>8</sub>PcH)Rh macrocycle.

As mentioned earlier, the X-ray structural data suggest that the N-H proton resides on a *meso* nitrogen. The chemical shift of  $\delta$  11.6 ppm for the N-H proton also indicates that the proton is highly deshielded and has to be on a *meso* nitrogen. For comparison, the N-H protons of R<sub>8</sub>PcH<sub>2</sub> are highly shielded and appear at  $\delta$  -0.201 ppm.

**(B) High Temperatures.** Figure 3 shows that both the Rh-H and the N-H resonances become narrower as the temperature is increased from 25 to ~45 °C, suggesting that there is a fast dynamic exchange process in this temperature range. Further increase in tem-

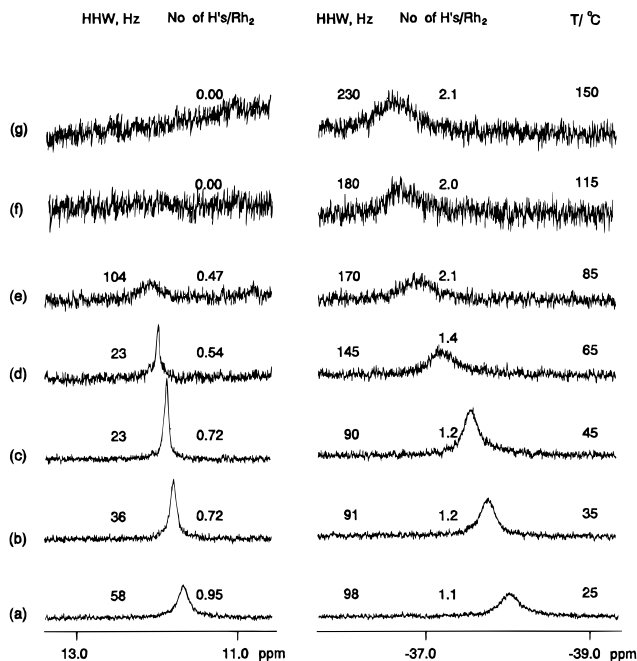


**Figure 3.** High-temperature <sup>1</sup>H NMR spectra of [(C<sub>5</sub>H<sub>11</sub>)<sub>8</sub>-PcRhH]<sub>2</sub> in toluene-*d*<sub>8</sub> in the N-H and Rh-H regions.  $P_{\text{H}_2} = 600$  mm Hg.

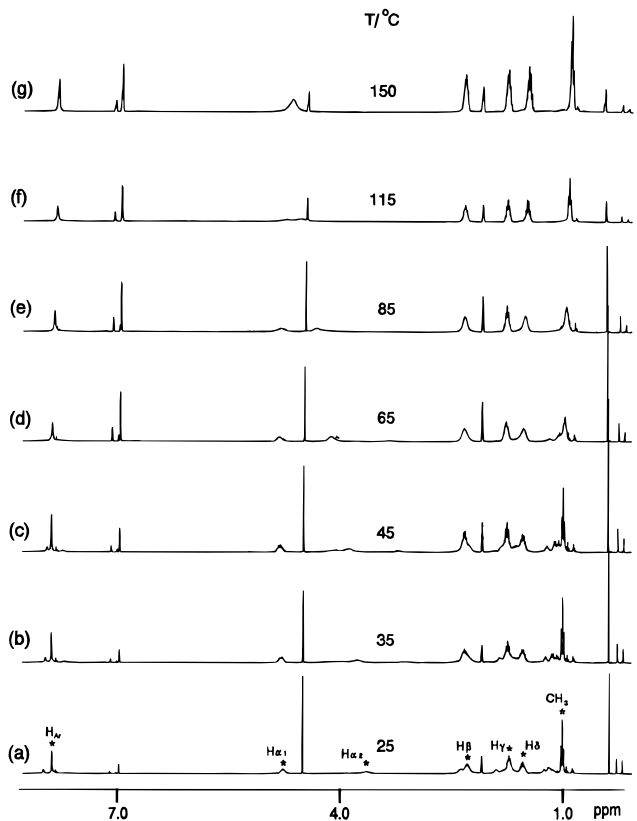


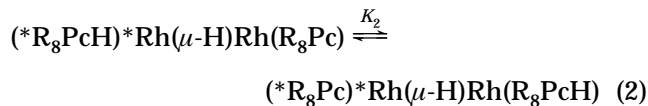
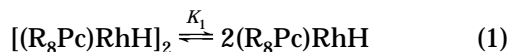
**Figure 4.** High-temperature <sup>1</sup>H NMR spectra of [(C<sub>5</sub>H<sub>11</sub>)<sub>8</sub>-PcRhH]<sub>2</sub> in toluene-*d*<sub>8</sub> in the alkyl-aryl region.  $P_{\text{H}_2} = 600$  mm Hg.

perature leads to broadenings of these resonances. Apparently, a new dynamic exchange process sets in at ~45 °C. In addition to the progressive broadening, the intensity of the Rh-H resonance increases at the expense of the N-H resonance, leading to the disappearance of the N-H resonance at 115 °C, at which there is one Rh-H resonance for each R<sub>8</sub>Pc<sup>2-</sup> ligand. At temperatures above 115 °C, the solution also gives

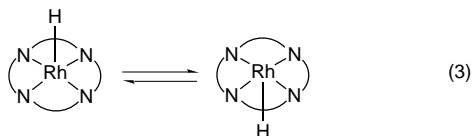
(7) (a) Lavallee, D. K.; Anderson, O. P. *J. Am. Chem. Soc.* **1982**, *104*, 4707. (b) Anderson, O. P.; Kopelove, A. B.; Lavallee, D. K. *Inorg. Chem.* **1980**, *19*, 2101. (c) Lavallee, D. K.; Kopelove, A. B.; Anderson, O. P. *J. Am. Chem. Soc.* **1978**, *100*, 3025. (d) Anderson, O. P.; Lavallee, D. K. *J. Am. Chem. Soc.* **1977**, *99*, 1404. (e) Goldberg, D. E.; Thomas, K. M. *J. Am. Chem. Soc.* **1977**, *99*, 913. (f) Grigg, R.; King, T. J.; Shelton, G. *J. Chem. Soc., Chem. Commun.* **1970**, 56.

(8) McLaughlin, G. M. *J. Chem. Soc., Perkin Trans. 2* **1974**, 136.

a very simple spectrum in the alkyl–aryl region. The hydrogens on each alkyl carbon, except for the  $\alpha$ -H's, appear as a multiplet, exhibiting their couplings to the neighboring H's, and all the aromatic H's appear as a singlet (Figure 4f,g). Apparently, **1** is converted to the monomeric  $(R_8Pc)RhH$  (**2**) when  $T \geq 115$  °C. The interconversion between **1** and **2**, as depicted in eq 1, has been observed previously when the solvent was changed between benzene and tetrahydrofuran.<sup>3</sup> This reversible dissociation-dimerization reaction provides a mechanism for the two macrocycles of **1** to become magnetically equivalent, as depicted in eq 2.

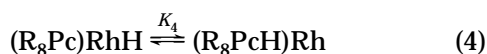


It should be noted that the two methylene H's on each of the pentyl carbons in **1**, as well as in **2**, are diastereotopic, as exemplified by the presence of two distinct resonances for the two  $\alpha$ -H's ( $\delta$  3.62 and 4.76 ppm) of the  $(R_8Pc)RhH$  macrocycle in **1** (Figure 4a).<sup>9</sup> These pairs of diastereotopic H's are made magnetically equivalent only if the dissociation and dimerization processes are interceded by transfer of the hydride ligand of **2** from one axial position to the other, as follows:



We believe that eq 1 is solely responsible for broadening the Rh–H and the N–H resonance as well as shifting the Rh–H resonance to lower field, in the temperature range of 45–115 °C (Figure 3c–g). Contribution by their dynamic exchange with H<sub>2</sub> or H<sub>2</sub>O can only be minimal, since neither resonance is significantly broadened.

The resonances for the two  $\alpha$ -H's of **2**, which appear at  $\delta$  4.7 and 4.9 ppm at 115 °C, merged into a broad singlet at  $\delta$  4.8 ppm at 150 °C. This may be attributed to equilibration of the two diastereotopic  $\alpha$ -H's of **2** via eq 3. We have not been able to record the spectra at higher temperatures, because the solution refluxes at temperatures above 150 °C. It appears that the Rh–H resonance continued to broaden as the temperature was raised beyond 115 °C. To account for the apparent broadening, we are proposing tautomerism between **2** and  $(R_8PcH)Rh$  (**3**), as depicted in eq 4, to rationalize this spectral change. The dynamic exchange between the two axial sites in eq 3 should not lead to a broad Rh–H resonance. It is very likely that **3** is a reaction intermediate in eq 3.



(9) The large separation of the two diastereotopic H's of  $\alpha$ -CH<sub>2</sub> is consistent with deshielding of these H's by two  $(R_8Pc)Rh$  macrocycles. For comparison, the two diastereotopic  $\alpha$ -H's of  $[(R_8Pc)Rh]_2$  appear at  $\delta$  3.9 and 4.9 ppm. See ref 3 for more discussion.

(10) Similar results in C<sub>6</sub>D<sub>6</sub>, presented in ref 3, reveal such spectral change more clearly.

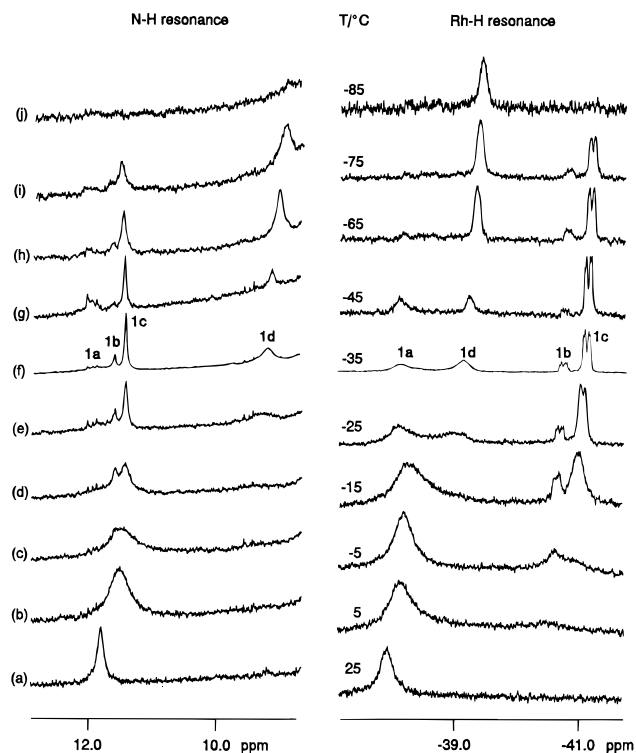


**Figure 5.** Low-temperature <sup>1</sup>H NMR spectra of  $[(C_5H_{11})_8\text{-PcRhH}]_2$  in toluene-*d*<sub>8</sub> in the N–H and Rh–H regions.

There are other features in Figure 4 that may not be explained by eq 1. As the temperature is increased from 25 °C, the resonances for the alkyl and the aryl H's of the  $(R_8PcH)Rh$  macrocycle first coalesce and then merge with the respective resonances of the  $(R_8Pc)RhH$  macrocycle. This occurrence might be attributed to migration of the proton among the four *meso* nitrogens. Such a migration of the proton would make all four benzene nuclei of  $(R_8PcH)Rh$  equivalent.

Equation 1 also fails to explain why both the N–H and the Rh–H resonances become sharper as the temperature is raised from 25 to 45 °C. Other dynamic processes that are observed in the low-temperature studies appear to be the cause; they are discussed in the next section.

**(C) Low Temperatures.** The <sup>1</sup>H NMR spectra of the solution of **1** in toluene-*d*<sub>8</sub> in the N–H and the Rh–H regions at +25 to –85 °C are shown in Figure 5. As the N–H and the Rh–H resonances for each spectrum in Figure 5 are plotted with the same expansion on both the vertical and the horizontal scale, the relative areas in each spectrum reflect the relative quantities of the N–H and the Rh–H moieties in the solution. This comparison may not be extended to resonances in different spectra collected at various temperatures, since the extent of precipitation of each of the Rh complexes in solution is unknown. Furthermore, each spectrum in Figure 5 is normalized to its most intense resonance.

The hydride resonances in Figures 5e–g clearly indicate the presence of four Rh–Hydride complexes. These four resonances are assigned to four different compounds, because their relative intensities change as the temperature is varied. One N–H resonance appears to be correlated with each of the four Rh–H resonances. Therefore, these four pairs of Rh–H and N–H resonances are assigned to the four isomers of **1** in Figure 1. These pairs of one-to-one correspondence are clearly

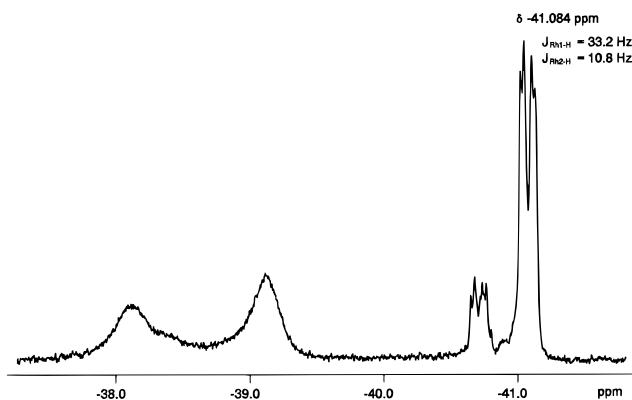


**Figure 6.** Hydride resonances of  $[(C_5H_{11})_8PcRhH]_2$  in toluene- $d_8$  at  $-35$  °C.

revealed in Figures 5e–i, and are marked in Figure 5f. At  $25$  °C, **1a** is the dominant species, and it is progressively converted to **1b**, **1c**, and **1d** as the temperature is lowered. The interconversions among these four isomers are reversible.

The assignment of the hydride-bridged isomer **1a** to **1** in the solid state has been discussed. It seems reasonable to assume that the dominant compound in benzene (and toluene) solutions at the ambient temperature is also **1a**, because it is less rigid than a terminal hydride dimer and should be favored at higher temperatures. The two isomers, the hydride resonances of which exhibit their couplings to two inequivalent Rh nuclei, are favored at low temperatures and are assigned to the pair of terminal hydride rotamers **1b** and **1c**. The last isomer, **1d**, which is the only isomer present in the solution at  $-85$  °C, is assumed to be a rotational isomer of **1a**.

The Rh–H and the N–H resonances of these four isomers only emerge as distinct resonances at  $-25$  °C. It can be derived from Figure 5f that the solution contains about 30% each of **1a**, **1c**, and **1d** and 10% of **1b** at  $-35$  °C. We believe that the sequence of exchange broadening, merging and subsequent narrowing of the Rh–H and N–H resonances of these isomers as the temperature was raised from  $-35$  to  $45$  °C is the result of interconversions among the four isomers.

At  $-25$  °C, the hydride resonances for **1a** and **1d** are broad, but those of **1b** and **1c** start to show fine Rh–H couplings, suggesting that only **1a** and **1d** are still quite active in slow dynamic exchange. It appears that the last exchange process that involves **1b** and **1c**, presumably their interconversion, is frozen out at  $-35$  °C. An expanded view of the hydride resonances at  $-35$  °C is shown in Figure 6. The hydride resonances for both **1b** and **1c** appear as a doublet of doublets, indicating that the hydrides are coupled to two inequivalent Rh nuclei. In support of these assignments, the N–H resonances for **1b** and **1c** are relatively sharp (HHW (half-height width) = 15 Hz for **1c**). In contrast, the Rh–H and N–H resonances for **1a** and **1d** remained broad at  $-45$  °C. It is likely that equilibration between the bridging-hydride isomers (**1a** and **1d**) and the terminal hydride isomers (**1b** and **1c**) proceeds through eq 1 and that these reactions are slower than the exchanges between **1a** and **1d** and between **1b** and **1c**.

It appears that, at  $-45$  °C, the dynamic exchange between **1a** and **1d** has been nearly frozen out. However, further cooling does not make their resonances any

sharper, and the Rh–H couplings for these isomers have never been observed. These results are attributed to broadenings of the resonances at lower temperatures because of increased viscosity of the solution. In support of this conclusion, the Rh–H couplings of the hydride resonance of **1b** and **1c** also started to collapse at  $-45$  °C and disappeared as the temperature was lowered to  $-65$  °C.

At  $-85$  °C, **1d** is the only isomer present, most likely because of selective precipitation of the other isomers, as well as shifts in equilibrium. Dark blue crystals were observed to deposit in the NMR tube. It is possible that, at temperatures below  $-75$  °C, **1a** is converted to **1d**, but **1b** and **1c** are precipitated out. Although the hydride resonance for **1d** is relatively narrow (HHW = 53 Hz), its N–H resonance is too broad to be observed. The much broader N–H resonance at low temperatures is attributed to its effective relaxation by the quadrupolar  $^{14}N$  nuclei.

## Discussion

We believe that isomer **1a** is the crystalline structure of **1** and is also the predominant isomer of its solution in benzene at ambient temperature. With the rigid square-planar phthalocyanine ligand, there are very few structures that can be formulated for the four isomers of **1**. We have, therefore, proposed that isomers **1b** and **1c**, which start to form from **1a** as the temperature is lowered to  $5$  °C, are the rotational isomers of the Rh–Rh-bonded dimers with a terminal hydride ligand. The last isomer, **1d**, is then assigned to a rotational isomer of **1a**. These assignments are partially based on the reasoning that the terminal hydride dimers are more rigid than the hydride-bridged dimers, **1a** and **1d**, and should be favored at lower temperatures as observed. The observation that the dynamic exchange between **1b** and **1c** is frozen out at about  $-25$  °C, while that between **1a** and **1d** is frozen out at  $-45$  °C is also consistent with the lower rotational barrier expected for the hydride-bridged dimers. On the basis of the intermediate rates of exchange calculated from Figures 5e–g,<sup>11</sup> the rotational barrier between **1a** and **1d** is estimated to be 3 kcal/mol. Presumably, the barrier comes from interference of the dangling pentyl groups with rotations around the two Rh–H bonds.

The schematic drawings for **1a** and **1d** in Figure 1 do not purport to show that the hydride ligand is on the Rh–Rh axis. As none of the known bridging hydride ligands of transition metals that have been located by neutron and X-ray diffraction studies<sup>12</sup> have been shown to reside on the metal–metal axis, it is most likely that the hydride ligand in **1a** and **1d** is also displaced from the metal–metal axis. With no data other than the X-ray diffraction data, which shows that the dimer assumes the  $35^\circ$ -staggered configuration in the solid state, we can only speculate that the dynamic exchange

(11) The frequency interval between **1a** and **1d** at  $-45$  °C is practically the same as that at  $-55$  °C and, therefore, is taken as the limiting value.

(12) (a) Bau, R.; Teller, R. G.; Kirtley, S. W.; Koetzel, T. F. *Acc. Chem. Res.* **1979**, *12*, 176. (b) Bullock, R. M.; Brammer, L.; Schultz, A. J.; Albinati, A.; Koetzel, T. F. *J. Am. Chem. Soc.* **1992**, *114*, 5125. (c) Albina, A.; Chaloupka, S.; Demartin, F.; Koetzel, T. F.; Kuegger, H.; Venanzi, L. M.; Wolfer, M. K. *J. Am. Chem. Soc.* **1993**, *115*, 169.

processes observed at low temperatures involve the equilibration between the staggered and the eclipsed rotamers.

On the basis of the observation that the aromatic H's of **1** in C<sub>6</sub>D<sub>6</sub> appear as four singlets in the ratio 1:1:2:4, we previously suggested<sup>3</sup> that the N–H proton resides on a pyrrolic nitrogen. In view of the structural evidence that all four pyrrolic nitrogens are practically identical in their bonding to the Rh nuclei and the NMR evidence that the N–H proton is highly deshielded, we now believe that the proton resides on a *meso* nitrogen. It is more likely that the 1:1:2:4 pattern was observed because two singlets of the expected 1:1:1:4 resonances of **1a** happen to have similar chemical shifts.

In contrast to a deshielding of the peripheral N–H protons, the diamagnetic ring current of the Pc ligand increases the shielding of protons residing inside the ring. Thus, the N–H resonance ( $\delta$  –0.20 ppm) of R<sub>8</sub>PcH<sub>2</sub> is shifted upfield by 8 ppm from that of pyrrole. Similarly, although the hydride resonances of Rh–Hydride complexes without an aromatic ligand appear in the range of  $\delta$  –7 to –22 ppm,<sup>13</sup> we have found that the hydride ligands of (R<sub>8</sub>Pc)(PMe<sub>3</sub>)RhH,<sup>14</sup> (R<sub>8</sub>Pc)(Py)–RhH,<sup>14</sup> and (R<sub>8</sub>Pc)RhH<sup>3</sup> are more shielded and appear at –21.22 (toluene-*d*<sub>6</sub>), –29.33 (toluene-*d*<sub>6</sub>) and –34.01 ppm (THF-*d*<sub>8</sub>), respectively. These data also show that change in the axial ligand L of the monomeric (R<sub>8</sub>Pc)–Rh(L)H complexes may cause the hydride resonance to shift as much as 13 ppm.

On the basis of the ring current effect alone, one may expect the resonances of the bridging hydrides in **1a** and **1d** to be 5–10 ppm upfield of those of the terminal hydrides in **1b** and **1c**. Therefore, it may be surprising that all these resonances appear within 3 ppm. Furthermore, the assignments, based mainly on the expected higher rigidity and higher rotational barrier for the terminal hydride dimers, actually put the hydride resonances of **1b** and **1c** upfield of **1a** and **1d**. As mentioned earlier, the bridging hydride ligand most likely resides off the Rh–Rh axis. Besides, the M–H bonds of bridging hydride ligands are usually about 0.20 Å longer than the corresponding terminal M–H bonds.<sup>12</sup> Both the longer M–H bond and the off-axis location of the hydride ligand reduce its shielding by the d electrons and by the induced magnetic field. Therefore, it seems possible that the upfield shift of the bridging hydride ligands in **1a** and **1d** is reduced so much as to be downfield of **1b** and **1c**.

The site of protonation of the protonated metallophthalocyanines has been the subject of several studies. Although the N–H proton was not located in the X-ray structural study of LuH(Pc)<sub>2</sub>,<sup>15</sup> protonation on a *meso* nitrogen was suggested because all the pyrrolic nitrogens are identically located in the structure. As mentioned earlier, N-alkylation of a porphyrin causes lengthening of the M–N bond, as well as tilting of the alkylated pyrrole ring.<sup>7</sup> Twigg<sup>16</sup> and Lever<sup>17</sup> also believed that protonation occurred on a *meso* nitrogen, on the basis

of the analysis of the electronic spectra. However, using the same technique, Harazono et al.<sup>18</sup> suggested that a pyrrolic nitrogen was the site of protonation in the solution of PcH<sub>2</sub> in trifluoroacetic acid. In the present study, both the X-ray diffraction and the <sup>1</sup>H NMR studies indicate that the N–H proton resides on a *meso* nitrogen. For Pc's and MPc's that form stable protonation products, the chemical shift of the N–H proton is a reliable diagnostic parameter to determine if the pyrrolic or the *meso* nitrogen is the site of protonation.

The observed  $\nu_{\text{N-H}}$  of 3367 cm<sup>–1</sup> for **1** suggests that the protonated nitrogen has much higher electron density than the ammonium ion or the iminium ion, the asymmetric N–H stretching vibrations<sup>19</sup> of which occur below 3200 cm<sup>–1</sup>. Apparently, the positive charge is delocalized over the extended  $\pi$  system rather than localized on the protonated *meso* nitrogen. The shifting of the charge density from the nitrogen to the carbon has also been used to explain the observation that the N–H bands of the guanidinium ions correspond to those of free amines rather than to the ammonium salts.<sup>19</sup>

## Experimental Section

**General Considerations.** All chemicals were reagent grade and were used without further purification. 1,4,8,11,15,18,22,25-Octapentylphthalocyanine, R<sub>8</sub>PcH<sub>2</sub>, was synthesized according to the method of Cook.<sup>20</sup> A General Electric GN300/89 NMR spectrometer, a Varian Unity 400 NMR spectrometer, and a Perkin-Elmer 660 FT IR spectrometer were used for spectral measurements. A Hewlett-Packard 5890 series II gas chromatograph was used for the GC analysis.

**X-ray Structure Determination and Refinement for [(R<sub>8</sub>Pc)RhH]<sub>2</sub>.**<sup>3</sup> A dark purple crystal deposited from the benzene solution of **1** was mounted on a pin and transferred to a Rigaku R-Axis II on a Ru-300 rotating anode generator. The space group was determined to be either centric C2/c or acentric Cc from systematic absences. The subsequent solution and successful refinement of the structure were carried out in the centric space group C2/c. A summary of the crystal data collection and refinement parameters is given in Table 1.

An ORTEP diagram of **1** is shown in Figure 2. High thermal motion was noted for the last two to four carbon atoms in each *n*-C<sub>5</sub>H<sub>11</sub> chain. Disorder was resolvable only for one carbon atom of the *n*-C<sub>5</sub>H<sub>11</sub> chains, which was refined in two positions at 50% occupancy each in alternate least-squares cycles. Only the first two or three carbon atoms in each chain (those exhibiting reasonable thermal motion) were refined anisotropically, as were Rh and the Pc ligand. Many of the pentyl chain atoms were refined isotropically due to disorder. The pentyl chains were refined with bond-length restraints such that bonded carbons were 1.55(1) Å and the nearest nonbonded neighbors were kept at 2.55(1) Å. Because of the high thermal motion and disorder, the hydrogen atoms were not included in the final refinement. Refinement of non-hydrogen atoms with anisotropic temperature factors (excepted as noted above) led to the final value of *R* = 0.078.

**Low-Temperature <sup>1</sup>H NMR Studies.** A solution of 2.0 mg of [(R<sub>8</sub>Pc)Rh]<sub>2</sub> and 15 mg of Cr(acac)<sub>3</sub> in 0.60 mL of toluene-*d*<sub>8</sub> was placed in a medium-walled NMR tube and freeze-pumped; H<sub>2</sub> at 600 mmHg was admitted. The sample was sealed with a flame and was then allowed to react in a 130 °C

(13) (a) Kaesz, H. D.; Saillant, R. B. *Chem. Rev.* **1972**, *3*, 231. (b) Thomas, K.; Osborn, J. A.; Powell, A. R.; Wilkinson, G. *J. Chem. Soc. A* **1968**, 1801.

(14) Unpublished data.

(15) Moussavi, M.; De Cian, A.; Fischer, J.; Weiss, R. *Inorg. Chem.* **1988**, *27*, 1287.

(16) Ledson, D. L.; Twigg, M. V. *Inorg. Chim. Acta* **1975**, *13*, 43.

(17) Bernstein, P. A.; Lever, A. B. P. *Inorg. Chim. Acta* **1992**, *198–220*, 543.

(18) Harazono, T.; Takagishi, I. *Bull. Chem. Soc. Jpn.* **1993**, *66*, 1016.

(19) Goto, T.; Nakanishi, K.; Ohashi, M. *Bull. Chem. Soc. Jpn.* **1957**, *30*, 723.

(20) Cook, M. J.; Daniel, M. F.; Harrison, K. J.; Mckeown, N. B.; Thompson, A. J. *J. Chem. Soc., Chem. Commun.* **1987**, 1086.

oven until the formation of  $[(R_8Pc)RhH]_2$  was complete. In order to obtain quantitative spectra in these experiments,  $Cr(acac)_3$  was added to the solution, and  $T_1$  measurements were conducted for each temperature so that change in the  $T_1$  value due to precipitation of  $Cr(acac)_3$  is properly corrected.

**Acknowledgment.** Support for this work was provided by the U.S. Department of Energy, Division of Chemical Sciences, Office of Basic Energy Sciences, under Contract No. W-31-109-ENG-38. X-ray diffraction data were collected at Molecular Structure Corp., The Woodlands, TX, as part of a product demonstration, and

we thank Dr. Bev Vincent for his assistance. We also thank Professor J. Halpern of the University of Chicago for helpful discussions.

**Supporting Information Available:** Tables giving atomic coordinates, bond distances and angles, and thermal parameters and figures showing the unit cell and crystal packing for **1** (10 pages). Ordering information is given on any current masthead page.

OM950908B